https://doi.org/10.17221/140/2024-SWR

Comparison of the cadmium and lead removal from three soils by electrokinetic remediation

Mei Zhang[1,2], Chengdong Duan[3], Xinfu Wang[1,2]*

[1]Jiangsu Design Institute of Geology for Mineral Resources (Testing Center of China National Administration of Coal Geology), Xuzhou, P.R. China
[2]Key Laboratory of Coal Measures and Mineral Resources, China Coal Geology Bureau, Xuzhou, P.R. China
[3]Xu Hai College of China University of Mining and Technology, Xuzhou, P.R. China

**Corresponding author: zhangmei@cumt.edu.cn*

Citation: Zhang M., Duan C.D., Wang X.F. (2025): Comparison of the cadmium and lead removal from three soils by electrokinetic remediation. Soil & Water Res., 20: 195–205.

Abstract: This study investigated, for the first time, the efficacy of citric acid (CA) and ethylenediaminetetraacetic acid (EDTA) as electrolytes in electrokinetic remediation (EKR) for removing lead (Pb) and cadmium (Cd) from three distinct soils (Anthrosols soil, AT; Acrisols soil, AC; and Chernozems soil, CH). Under a voltage gradient of 2 V/cm and a remediation duration of 4 days, EDTA proved most effective for Anthrosols, achieving removal rates of 17.8% for Cd and 12.8% for Pb-lower than those observed for Acrisols and Chernozems, likely due to AT's high pH background. These results suggest that combining EKR with other remediation techniques could enhance efficiency for such soils. For Acrisols soil, extending the remediation time to 10 days significantly improved metal removal: Cd removal reached 91.1% with CA, while Pb removal attained 62.7% with EDTA. Chernozems soil exhibited higher sensitivity to EKR, with pronounced focusing phenomena. In CH1, Cd removal in anode-proximal (S1) zone reached 99%, but accumulation in the cathode-adjacent (S4 and S5) reduced the average removal rate to 22%, indicating the potential for improvement through cathodic control. Similarly, in CH2, Pb removal in S5 achieved 84.8%, while focusing in S1 suggested the need for anodic optimisation. These findings highlight the influence of soil properties and operational parameters on EKR efficiency, providing insights for tailored remediation strategies.

Keywords: electrokinetic remediation; lead-cadmium; three soils

Soil pollution in China was extensive and severe, with inorganic contaminants being the primary cause. Nationwide, the soil exceedance rate reaches 16.1%, with pollution levels in southern regions surpassing those in the north. Heavy metals like Cd, Hg, As, and Pb exhibited increasing concentrations from northwest to southeast and northeast to southwest. To better understand spatial distribution, researchers have developed detailed geochemical maps correlating heavy metal concentrations with precise geographic coordinates (Duan et al. 2016). Given the severe risks posed by heavy metals to public health and ecosystems (Zhang et al. 2012; Luo & Teng 2020), effective remediation strategies are urgently needed.

Various techniques, including soil washing, chemical oxidation, bioremediation, and phytoremediation, have been explored (Chung & Lee 2007; Yeung & Gu 2011; Zulfiqar et al. 2017). However, they were often

Supported by the Xuzhou City Science and Technology Project Special Fund (Grant No. KC21334) and the Jiangsu Provincial Science and Technology Program (Grant No. BE2023855).

https://doi.org/10.17221/140/2024-SWR

found to be costly, energy-intensive, and ineffective, and they could create other adverse environmental impacts. Electrochemical remediation has unique advantages over other conventional technologies, including applicability to low-permeability and heterogeneous soils (Chung & Lee 2007; Yeung & Gu 2011; Hu et al. 2023), flexibility to use as ex-situ or in situ method, and easy integration with conventional technologies, which was an effective and promising remediation technology for heavy metal complex contaminated soils (Acar & Alshawabkeh 1993; Yeung & Gu 2011).

Soil properties, electric field characteristics, electrolyte components, and enhancements influenced electrokinetic remediation efficacy. Control of electrolyte addition or pH was still the primary measure to enhance the electrokinetic remediation effect at the laboratory and field scales (Benamar et al. 2020). Ethylenediaminetetraacetic acid (EDTA) was the most commonly used chelating agent because of its high chelating ability for heavy metals, low impact on soil properties, slow degradation by microorganisms, etc. (Giannis & Gidarakos 2005; Villen-Guzman et al. 2015; Song et al. 2016). Citric acid was a small molecule organic acid that can increase the electroosmotic flow during the electrokinetic remediation process (Cameselle 2015; Xie et al. 2021) and can form complexes with Cd and Pb, was relatively inexpensive and easy to handle (Bassi et al. 2000). Thus, EDTA and citric acid were quality candidates for enhanced electrokinetic remediation. Soil heterogeneity had a significant influence on the electrokinetic remediation of heavy metal-contaminated soils (Appel & Ma 2002; Ottosen et al. 2006; Peng et al. 2018). Due to the variability of soil-forming factors (climate, parent material, biology, topography, time, and human activities), soil distribution had zonal regularity, resulting in significant variability of soil physicochemical properties between southern and northern China. Researchers had studied electrokinetic remediation of heavy metal-contaminated soil for extended periods. They found that the removal of Pb and Cd in Chernozems was 95.85% and 98.44% under a steady potential gradient of 1 V/cm and running time of 705 h when the electrolyte was 0.2 M citric acid mixed with 0.05 M $CaCl_2$ (Yuan et al. 2017); Researchers showed that the removal rate of Cd in Acrisols could reach 79.18% after 96 h of electrokinetic remediation (Zhou et al. 2004). It was impossible to directly compare the removal of contaminants due to the inconsistency of experimental conditions (like electrolyte type, running time, and soil type).

This study investigated the effects of CA and EDTA as electrolytes in EKR for three distinct soils – Chernozems (CH), Acrisols (AC), and Anthrosols (AT) – contaminated with Pb and Cd. We analysed the influence of soil physicochemical properties on removal efficiency and explore the migration patterns and underlying mechanisms of heavy metals during EKR.

MATERIAL AND METHODS

Soil. The sampling locations were schematically illustrated in Figure 1. The Acrisols (AC) were collected from Jiujiang City, Jiangxi Province, a subtropical transitional zone characterised by abundant water and heat resources, leading to intense chemical and physical weathering. The Anthrosols (AT) were obtained from Xuzhou City, Jiangsu Province, situated in a mid-latitude warm-temperate monsoon climate region. The Chernozems (CH) were sampled from Harbin City, Heilongjiang Province, located in the northern temperate zone under a temperate monsoon climate. Soil samples were air-dried naturally, and plant residues and stones were removed before sieving through a 10-mesh sieve. To prepare Pb-Cd composite contaminated soil, predetermined amounts of analytical-grade $Pb(NO_3)_2$ and $Cd(NO_3)_2$ were dissolved in deionised water and thoroughly mixed with the soil. The mixture was then equilibrated for one month. The physicochemical properties of the artificially contaminated soils were summarised in Table 1.

Experimental setup. The experimental setup, illustrated in Figure 2, was constructed from plexiglas and comprised two main compartments: a soil chamber (L × H × W = 25 × 10 × 10 cm) and two electrode chambers (L × H × W = 6 × 15 × 15 cm). The two compartments were separated by a removable porous Plexiglas plate and filter paper. Sampling ports were positioned above the soil chamber, while gas produced during electrolysis was vented from the top of the electrode chamber.

To enhance the practical applicability of laboratory results, soil sample pretreatment was minimized. A 4 000 g prepared soil sample was compacted into the soil chamber. The electrolyte was added to both anode and cathode chambers, maintaining the liquid level at the same height as the soil column. A constant voltage gradient of 2 V/cm was applied throughout

https://doi.org/10.17221/140/2024-SWR

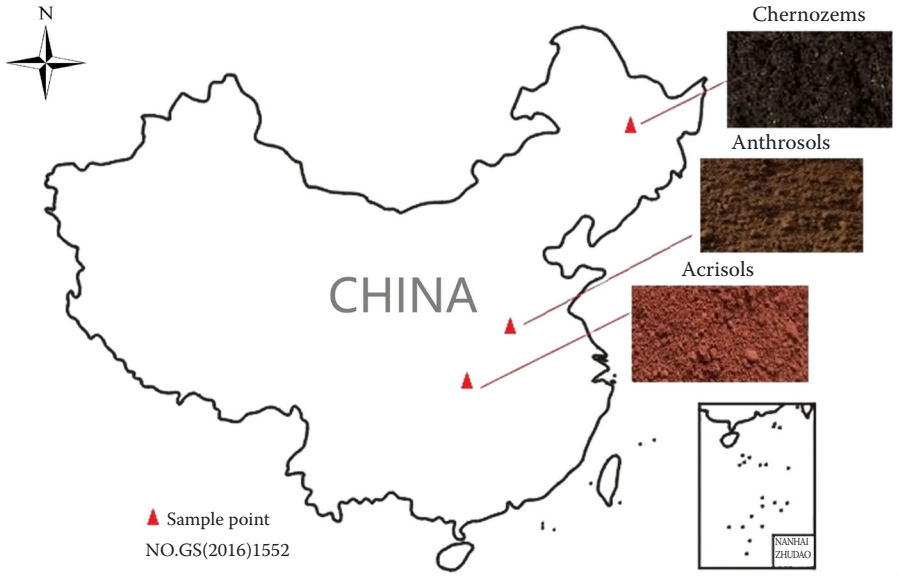

Figure 1. Schematic diagram of sampling points

Table 1. Physical and chemical characteristics of the tested sediment

Soils	Anthrosols	Acrisols	Chernozems
pH	7.69	5.23	6.59
Cd (mg/kg)	89.4	88.9	90.1
Pb (mg/kg)	694.3	702.8	697.2
Organic matter	10.3	3.85	30.4
Fe_2O_3 (%)	4.34	8.02	4.76
CaO (%)	0.83	0.32	0.98
Cation exchange capacity (cmol/kg(+))	26.5	26.4	26.8

the experiment. During the treatment process, the electric current and pH values in both electrode chambers were monitored daily. Upon completion, the treated soil was sectioned into five equal segments along the anode-to-cathode axis (designated as S1 through S5). Each segment was analysed for pH

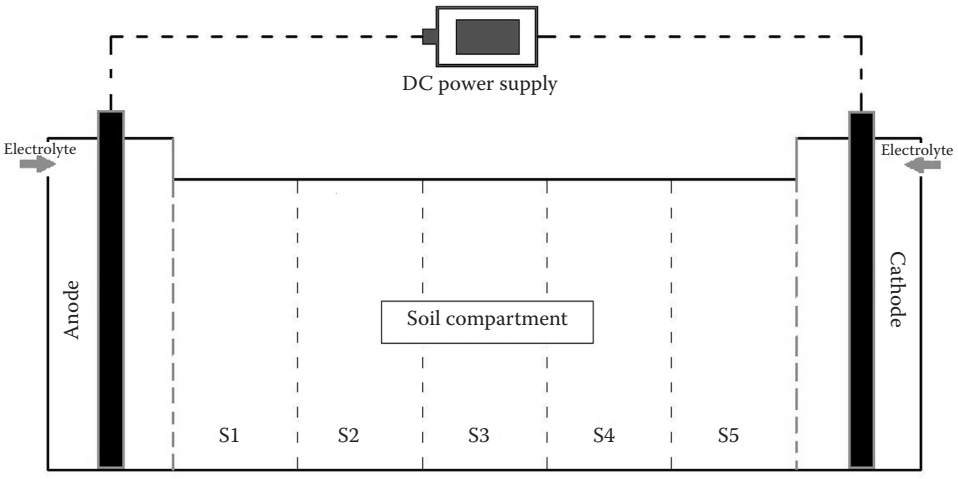

Figure 2. Schematic diagram of the experimental setup
S1–S5: along the anode-to-cathode axis of the treated soil (designated as S1 through S5)

https://doi.org/10.17221/140/2024-SWR

Table 2. Operating parameters in tests

Test	Anolyte	Catholyte	Voltage gradient (V/cm)	Time (days)
AT0, AC0, CH0	deionised water	deionised water	2	10
AT1, AC1, CH1	0.3 mol/L CA	0.1 mol/L CA	2	10
AT2, AC2, CH2	0.05 mol/L EDTA	0.05 mol/L EDTA	2	10

CA – citric acid; EDTA – ethylenediaminetetraacetic acid; AT – Anthrosols; AC – Acrisols; CH – Chernozems

and heavy metal content. The detailed experimental conditions are summarised in Table 2.

Analysis method. Soil pH was measured via potentiometry (ISO 10390:2005), and cation exchange capacity (CEC) was determined by ammonium acetate displacement (ISO 11260:2017). Organic matter content was quantified using the potassium dichromate oxidation method (ISO 10694:1995), while cadmium (Cd) concentrations were analysed by graphite furnace atomic absorption spectrometry (ISO 11047:1998). The contents of calcium oxide (CaO), iron(III) oxide (Fe_2O_3), and lead (Pb) were determined following the inductively coupled plasma optical emission spectrometry (ICP-OES) procedures outlined in ISO 11885:2007.

RESULTS AND DISCUSSION

Soil pH. The electrochemical remediation process involved distinct redox reactions at the electrodes. At the anode surface, oxidation reactions generated H^+ ions, which subsequently migrated through soil pores to the cathode via multiple transport mechanisms, including electromigration, electroosmosis, and concentration gradient-driven diffusion. Conversely, reduction reactions at the cathode surface produced OH^- ions, which participated in two key processes: (1) neutralisation reactions, and (2) precipitation and reduction of heavy metal ions. These electrode reactions induced significant pH changes in the electrolyte solutions (Figure 3). The anolyte pH exhibited substantial decreases to 2.23, 1.66, and 3.16 when using distilled water, citric acid, and EDTA as electrolytes, respectively. Correspondingly, the catholyte pH increased to 11.6, 3.35, and 9.05 for these same electrolytes.

The spatial variation in soil pH was predominantly governed by electrolyte diffusion processes and H^+ electromigration, as illustrated in Figure 4. Under deionized water electrolyte conditions, AT0 soil exhibited a pronounced pH gradient, with the anode-proximal S1 zone decreasing from an initial pH of 7.69 to 4.86, while the cathode-adjacent S5 zone increased to 8.71. Similarly, AC0 soil demon-

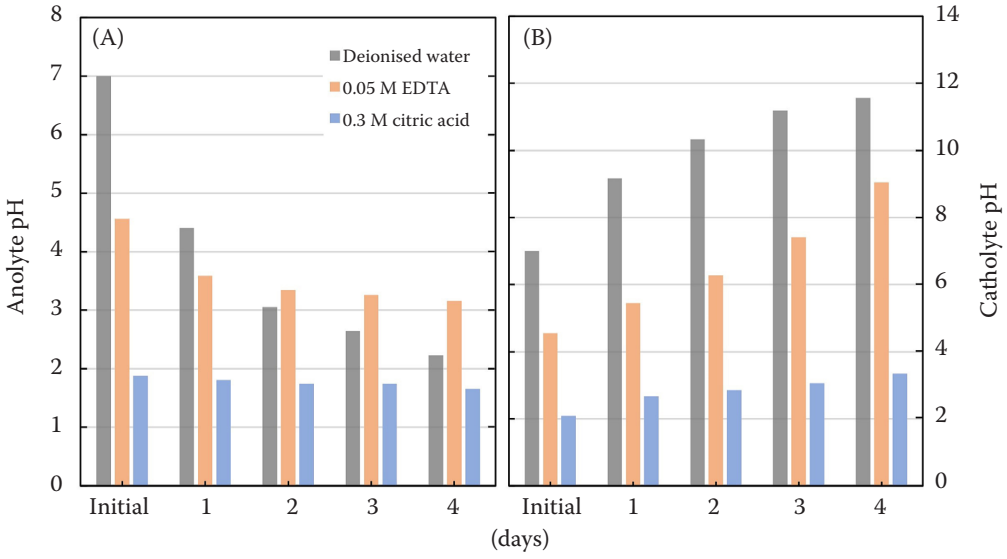

Figure 3. The pH change of catholyte and anolyte during electrokinetic remediation
EDTA – ethylenediaminetetraacetic acid

https://doi.org/10.17221/140/2024-SWR

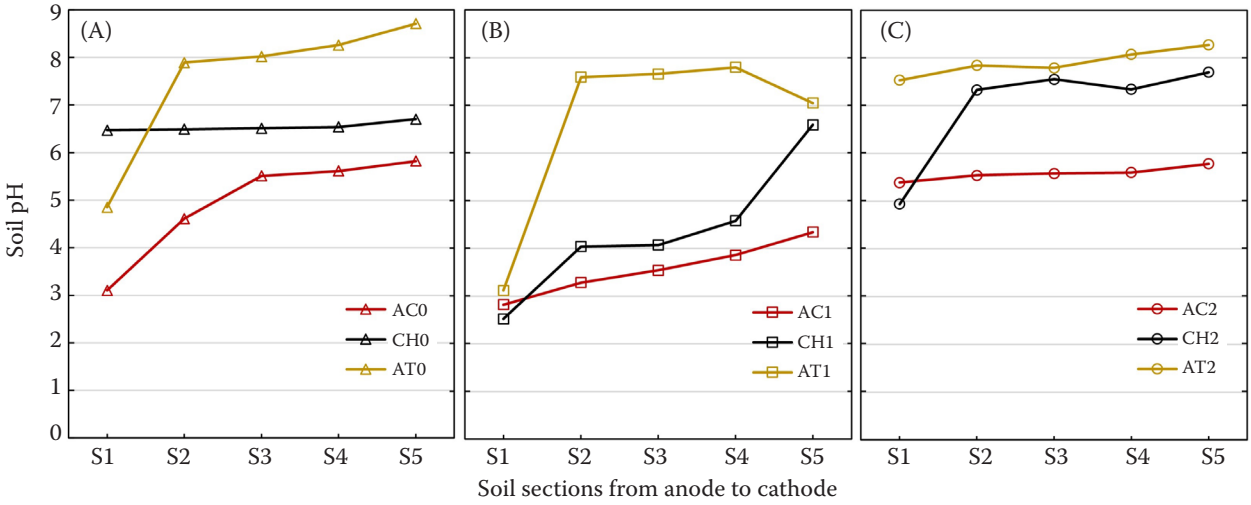

Figure 4. Spatial variation of soil pH profiles following 4-day electrokinetic remediation treatment
AC – Acrisols; CH – Chernozems; AT – Anthrosols; AC0, CH0, AT0 – deionised water treatment; AC1, CH1, AT1 – citric acid enhanced treatment; AC2, CH2, AT2 – ethylenediaminetetraacetic acid enhanced treatment

strated analogous trends, with S1 pH decreasing from 5.21 to 3.1 and S5 increasing to 5.82. In contrast, CH0 soil (initial pH 6.59) maintained relatively stable pH values in both S1 and S5 zones throughout the remediation process. When citric acid served as the electrolyte, AT1 soil displayed enhanced acidification in the S1 zone (pH 3.12), with catholyte diffusion causing a moderate pH reduction to 7.05 in S5. More dramatic pH alterations were observed in CH1 and AC1 soils, particularly in CH1, where S1 pH plummeted to 2.52 and S2-S4 zones experienced substantial acidification (pH 4.0~4.6), while S5 remained essentially unchanged. EDTA application induced distinct pH response patterns, with all tested soils (AT2, AC2, CH2) showing progressive pH increases across S1–S5 zones. Notably, CH2 soil exhibited the most significant pH elevation in S2–S4 zones, suggesting enhanced buffering or complexation mechanisms. Comparative analysis revealed three key findings: (1) AT soil's stable S2–S4 pH profile (ΔpH < 0.6) confirmed its inherent buffering capacity; (2) CH soil demonstrated marked electrolyte sensitivity, with S2–S4 pH variations exceeding 1.6 units across treatments; and (3) AC soil's acidic nature rendered it particularly susceptible to citric acid-induced acidification (ΔpH up to 2.4), while showing limited response to EDTA (ΔpH < 0.6). These differential responses highlight the critical role of both soil properties and electrolyte composition in determining pH evolution during electrochemical remediation.

Variation of current. The electrical current magnitude exhibited a strong positive correlation with the concentration of mobile ions in soil pore water (Acar & Alshawabkeh 1993; Wang et al. 2021), as evidenced by the current variation profile presented in Figure 5. The current dynamics followed a characteristic pattern: an initial increase phase followed by a gradual decline. During the early experimental stage, the dissolution of water-soluble soil compounds into pore water, coupled with H^+-mediated ion displacement reactions, led to progressively increasing mobile ion concentrations and consequently, rising current values. Subsequent current reduction resulted from two concurrent processes: (1) electromigration of charged species toward respective electrodes, depleting mobile ions in pore water, and (2) precipitation reactions between cathodically generated OH^- and metal ions (Ca^{2+}, Mg^{2+}, Fe^{3+}) as reported by Li et al. (2020). These precipitation products accumulated in soil pores, increasing overall soil resistance and contributing to the current decline. Comparative analysis of Figure 5B, C revealed significantly higher current magnitudes in CH1 and CH2 samples relative to their experimental counterparts. This observation suggests enhanced ion mobility in CH soil aqueous phases, attributable to two key factors: (1) more pronounced pH modification effects in CH soil systems, and (2) greater ion desorption from soil matrix components under these conditions. The current profiles thus serve as effective indicators of both ion mobility dynamics

https://doi.org/10.17221/140/2024-SWR

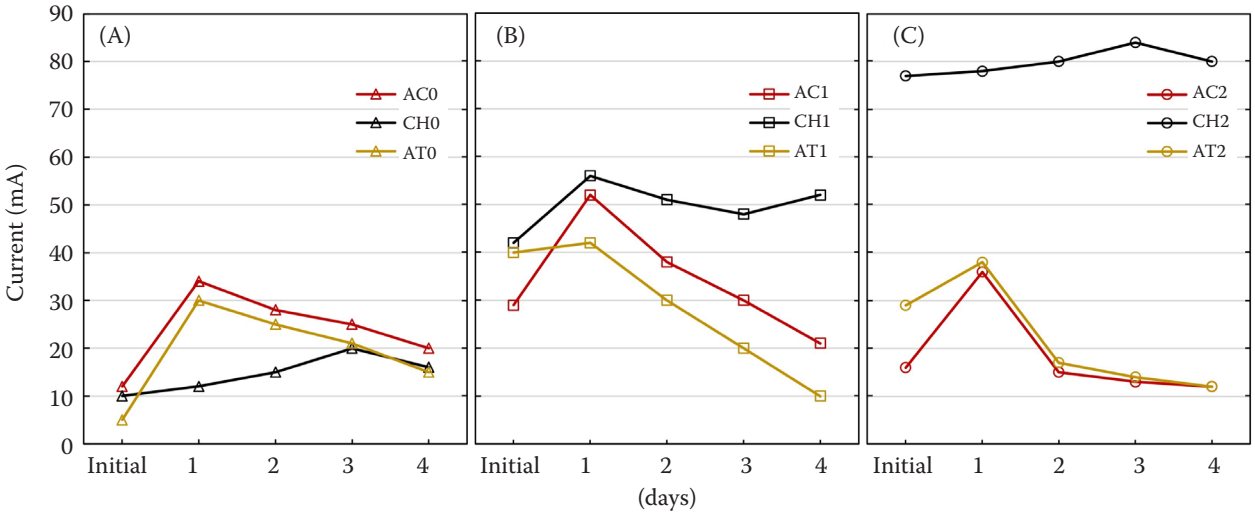

Figure 5. Current change during electrokinetic remediation

AC – Acrisols; CH – Chernozems; AT – Anthrosols; AC0, CH0, AT0 – deionised water treatment; AC1, CH1, AT1 – citric acid enhanced treatment; AC2, CH2, AT2 – ethylenediaminetetraacetic acid enhanced treatment

and soil-specific electrochemical responses during remediation processes.

Pb, Cd removal. During electrokinetic remediation, H^+ migration toward the cathode facilitated continuous ion exchange reactions with cationic pollutants. Concurrently, electroosmotic flow and concentration-driven diffusion of pore fluids transported heavy metals toward the cathode, enabling effective pollutant removal (Gent et al. 2004). Figure 6 presents the spatial distribution of cadmium residual rates following electrokinetic treatment. Initial remediation tests with deionised water (Figure 6A) revealed distinct soil-specific responses: AT0, AC0, and CH0 exhibited average Cd residual rates of 97.3%, 81.6% and 94%, respectively, with AC0's S1 zone showing the most pronounced removal (44.9% residual). The citric acid-enhanced treatment (Figure 6B) demonstrated progressive increases in Cd residuals from S1 to S5 zones in AC1 (average 66.2%), with remarkably efficient removal in the acidic S1 zone (pH 2.8, 17.8% residual). Comparative analysis confirmed significantly enhanced removal efficiency versus controls,

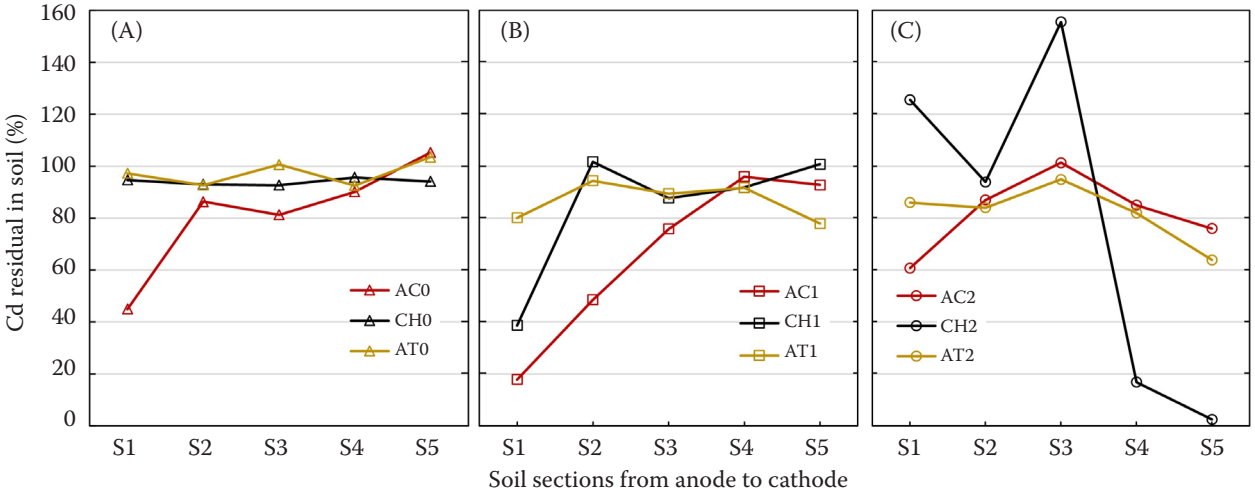

Figure 6. Cd residue rate in soil after 4 days of remediation

AC – Acrisols; CH – Chernozems; AT – Anthrosols; AC0, CH0, AT0 – deionised water treatment; AC1, CH1, AT1 – citric acid enhanced treatment; AC2, CH2, AT2 – ethylenediaminetetraacetic acid enhanced treatment

https://doi.org/10.17221/140/2024-SWR

particularly in S1 zones across all soil types. These results establish soil pH as a critical determinant of Cd removal efficiency when using deionised water or citric acid electrolytes, with lower pH correlating strongly with higher removal rates. However, EDTA-mediated remediation (AT2, AC2, CH2 averages: 82.1%, 82.0%, 78.8% respectively) showed reduced pH dependence, instead producing a characteristic "low-high-low" residual profile with metal accumulation in central zones (S3). Notably, CH2 exhibited exceptional removal in cathode-proximal zones (S5: 2.4%, S4: 16.8%), suggesting enhanced formation of mobile anionic Cd-EDTA complexes (e.g., $[Cd\text{-}EDTA]^{2-}$) that migrated toward the anode under electric fields, as documented by Villen-Guzman et al. (2015) and Song et al. (2016).

Figure 7 presents the spatial distribution of lead removal rates following electrokinetic remediation. The control group (Figure 7A) demonstrated limited Pb removal, with AC0 showing the lowest residual rate of 84.1% in the acidic S1 zone (pH = 3.1), while maintaining exceptionally high residuals (91.8% average) in S2–S5 zones. Citric acid-enhanced remediation (Figure 7B) yielded improved results, with AC1 exhibiting the lowest average Pb residual (80.0%) among the tested soils. Notably, removal efficiencies followed pH gradients: S1 (60.9% at pH = 2.82) > S2 (82.1% at pH = 3.28) > S4–S5 (84.3–84.5% at pH = 3.86–4.34), with clear metal accumulation in the S3 zone. This spatial pattern, combined with the enhanced removal at lower pH values, confirms the formation of mobile anionic Pb-citrate complexes (e.g., Pb-$(citrate)_2^{4-}$) that migrate toward the anode, as well as the critical pH threshold (< 4) for effective Pb desorption from soil matrices (Li et al. 2014). EDTA-mediated remediation (Figure 7C) revealed distinct transport mechanisms, with AT2 and CH2 showing metal accumulation in central zones (S3) and AC2 in S1, while all systems exhibited minimum residuals in cathode-proximal zones (S5 < S4). The particularly pronounced removal in CH2 (S5 residual < 10.8%) demonstrates that at higher pH (> 5.7), EDTA predominantly facilitates Pb removal through formation of stable anionic complexes (e.g., $[Pb\text{-}EDTA]^{2-}$), consistent with previous reports (Villen-Guzman et al. 2015; Chen et al. 2025). These results systematically demonstrated how electrolyte chemistry and soil pH jointly control Pb speciation and electromigration behaviour during electrokinetic remediation.

Comparative analysis revealed significantly lower removal efficiencies for both Pb and Cd in AT soil compared to AC and CH soils, attributable to multiple interacting factors. Firstly, the AT soil exhibited strong buffering capacity that maintained relatively stable pH conditions during remediation (Figure 4), thereby limiting the pH-dependent processes critical for heavy metal mobilization, including mineral dissolution, pollutant desorption, and solid-liquid phase ion exchange (López Vizcaíno et al. 2018). Secondly, AT's elevated organic matter content facilitated strong metal retention through multiple binding mechanisms: (1) electrostatic adsorption,

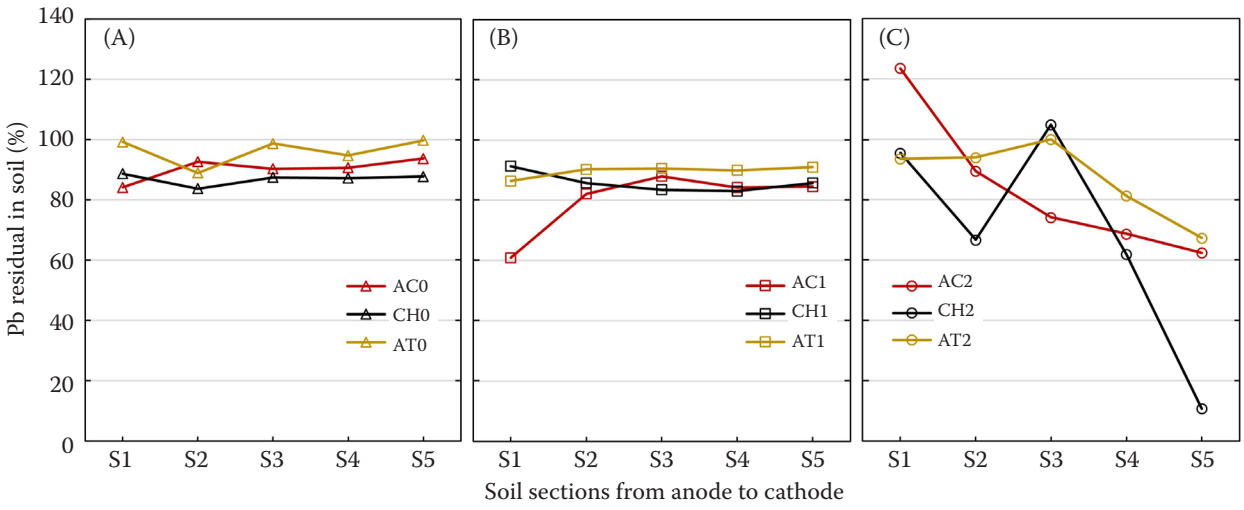

Figure 7. Pb residue rate in soil after 4 days of remediation

AC – Acrisols; CH – Chernozems; AT – Anthrosols; AC0, CH0, AT0 – deionised water treatment; AC1, CH1, AT1 – citric acid enhanced treatment; AC2, CH2, AT2 – ethylenediaminetetraacetic acid enhanced treatment

https://doi.org/10.17221/140/2024-SWR

(2) complexation/chelation reactions forming insoluble metal-organic complexes (Peng et al. 2018), and (3) synergistic interactions between pH and organic matter that enhanced metal fixation beyond what either factor could achieve independently (Hou et al. 2019). Additional contributing factors included AT's distinct cation exchange capacity and redox characteristics that collectively influenced metal mobility. These findings demonstrate that AT's combination of strong pH buffering capacity, organic-rich matrix, high pH background, and multifactorial metal retention mechanisms significantly constrained electrokinetic remediation effectiveness. To overcome these limitations, we recommend integrating electrokinetics with complementary approaches such as: (1) chemical leaching (Giannis & Gidarakos 2005; Ng et al. 2014), (2) permeable reactive barriers (Chung & Lee 2007; Zhang et al. 2012), or (3) targeted chemical amendments (Murtaza et al. 2011; Zulfiqar et al. 2017).

Extended remediation impact on Cd and Pb removal. The remediation duration significantly influenced the migration of ionic species and the desorption/dissolution of contaminants in the soil (Diagboya et al. 2015). Due to the directional migration of H^+ ions – aligned with electroosmotic flow – their effective mobility was enhanced, resulting in a migration rate approximately 2 times faster than that of OH^-. Consequently, prolonged remediation led to a pronounced decrease in soil pH across most zones. Table 3 and Figure 8 illustrate the enhanced removal efficiencies for Cd and Pb after 10 days of remediation in AC and CH soils. In the citric acid-enhanced system (AC1), remarkable Cd removal was achieved with an average efficiency of 91.1%, showing spatial variation from 99.5% in the strongly acidic S1 zone (pH = 2.43) to 69.1% in S5. The CH1 system displayed a distinct pH gradient ranging from 2.21 (S1) to 7.98 (S5), corresponding to decreasing Cd removal efficiencies from 99% (S1) to < 66% (S3), with significant metal accumulation (focusing) observed in higher pH zones (S4–S5) where hydroxide precipitation occurred due to cathodic OH^- migration. EDTA-mediated systems (AC2 and CH2) demonstrated different transport mechanisms, with both showing almost identical average Cd removal and consistent spatial patterns (S5 > S4 > S3 > S1 > S2). This distribution reflected pH-dependent speciation changes: at pH < 4.5 (S1), cationic Cd^{2+} migrated toward the cathode, while in higher pH zones (S3–S5), anionic $[Cd\text{-}EDTA]^{2-}$ complexes formed and migrated toward the anode, accumulating in S2. These findings suggest two optimisation strategies: (1) maintaining acidic conditions (< pH 4) to enhance Cd^{2+} mobility, and (2) implementing anolyte pH control to minimise focusing effects during EDTA-enhanced remediation.

The Pb removal efficiencies exhibited significant variation between soil types and treatment conditions. In citric acid-enhanced systems, AC1 achieved 40.3% average Pb removal with maximum efficiency in the acidic S1 zone (84.8%), while CH1 showed

Table 3. Cd and Pb removal after 10-day electrokinetic remediation (in %)

Test	AC0	AC1	AC2	CH0	CH1	CH2
Cd						
S1	92	99.5	49	3	99	23
S2	23	99	–5	15	90	–33
S3	19	98	50	6	66	50
S4	17	90	64	9	–64	87
S5	–14	69	90	12	–82	90
Pb						
S1	30.5	84.8	41.3	14.8	54.9	–13
S2	12.1	69.9	56.5	20.2	9.4	15.6
S3	9.1	30.7	63.6	15	7.6	57.7
S4	12	11.9	55.5	14.4	12.3	67.1
S5	4	4	96.4	18.9	15.7	84.8

S1–S5 – soil sections from anode to cathode; AC – Acrisols; CH – Chernozems; AC0, CH0 – deionised water treatment; AC1, CH1 – citric acid enhanced treatment; AC2, CH2 – ethylenediaminetetraacetic acid enhanced treatment

https://doi.org/10.17221/140/2024-SWR

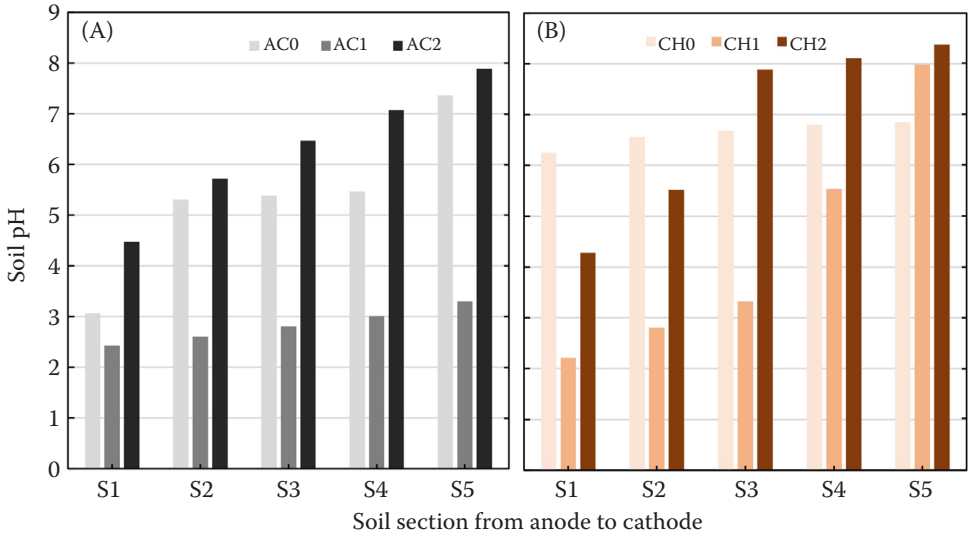

Figure 8. Spatial variation of soil pH profiles following 10-day electrokinetic remediation treatment
AC – Acrisols; CH – Chernozems; AC0, CH0 – deionised water treatment; AC1, CH1 – citric acid enhanced treatment; AC2, CH2 – ethylenediaminetetraacetic acid enhanced treatment

lower overall removal (20%) with peak efficiency of 54.9% in S1. Both systems displayed minimal removal in higher pH zones (AC1-S5: 4%; CH1-S3: 7.6%), demonstrating the combined influence of three key factors: (1) soil pH gradients, (2) organic matter content, and (3) Pb speciation and complexation dynamics with electrolyte components. Notably, Pb removal in AC1 (40.3%) was substantially lower than concurrent Cd removal (91.1%), attributable to Cd's weaker competitive adsorption capacity and consequent ease of displacement into mobile phases. EDTA-mediated systems revealed different behaviour patterns: AC2 demonstrated improved average Pb removal (62.6%) with a consistent decreasing gradient from S5 to S1, while CH2 showed moderate removal (42%) with metal accumulation in S1. This performance discrepancy between soils reflected their fundamental differences – CH's higher native pH (6.59 vs AC's 5.21) and elevated organic content (30.4 g/kg vs AC's 3.85 g/kg) promoted the formation of stable Pb-organic chelates that resisted desorption and mobilisation.

Comparative analysis revealed distinct remediation mechanisms between citric acid and EDTA as electrolytes for Pb and Cd removal. Citric acid primarily functioned through two synergistic pathways: (1) progressive soil acidification that enhanced metal desorption from soil particles, and (2) formation of mobile anionic metal-citrate complexes. This dual mechanism proved particularly effective for Cd removal, achieving significantly higher efficiencies than for Pb. In contrast, EDTA predominantly operated through strong chelation, forming stable anionic complexes such as $[Pb\text{-}EDTA]^{2-}$ that facilitated electromigration. This complexation-driven mechanism demonstrated superior performance for Pb removal compared to Cd, as evidenced by the higher Pb mobilization rates in EDTA-enhanced systems. The differential effectiveness of these electrolytes highlights the importance of ligand-specific interactions in electrokinetic remediation, where citric acid's acidification capacity favours Cd mobilisation while EDTA's chelation strength preferentially enhances Pb removal.

CONCLUSION

(1) For Anthrosols soil with alkaline characteristics (pH 7.69), electrokinetic remediation at 2 V/cm for 4 days showed limited effectiveness, with optimal removal rates of only 17.8% for Cd and 12.8% when using EDTA as electrolyte. The high buffering capacity and organic matter content of AT soil significantly constrained remediation efficiency, suggesting the need for combined remediation approaches integrating electrokinetics with other techniques.

(2) Acrisols soil demonstrated excellent remediation potential due to its acidic nature (pH 5.21) and

https://doi.org/10.17221/140/2024-SWR

low organic content. Extended treatment duration (10 days) achieved remarkable removal efficiencies: 91.1% for Cd with citric acid electrolyte and 62.7% for Pb with EDTA, establishing it as the most suitable candidate for electrokinetic remediation among the tested soils.

(3) Chernozems soil exhibited complex remediation dynamics owing to its high organic matter content (30.4 g/kg). While exceptional Cd removal (99%) occurred in acidic zones (S1, pH 2.21), severe focusing phenomena in S4–S5 regions reduced average removal to 22%, necessitating cathodic control measures. Similarly, for Pb, though S5 achieved 84.8% removal, anode-proximal accumulation in S1 indicated the importance of anodic pH regulation in organic-rich soils.

(4) Pre-remediation assessment of soil characteristics and contamination profiles is critical for electrolyte selection. Citric acid proves optimal for Cd-dominated contamination through its dual acidification and complexation effects, while EDTA shows superior performance for Pb pollution via stable chelate formation ($[Pb\text{-}EDTA]^{2-}$). This selective approach maximizes remediation efficiency based on primary contaminant identity and soil physicochemical properties.

Acknowledgements. The authors would like to extend their thanks to the providers of the materials used in this study and their appreciation to CUMT, which offered support for this study.

REFERENCES

Acar Y.B., Alshawabkeh A.N. (1993): Principles of electrokinetic remediation. Environment Science &Technology, 13: 2638–2647.

Appel C., Ma L. (2002): Concentration, pH, and surface charge effects on cadmium and lead sorption in three tropical soils. Journal of Environment Quality, 31: 581–589.

Bassi R., Prasher S.O., Simpson B.K. (2000): Extraction of metals from a contaminated sandy soil using citric acid. Environmental Progress, 4: 275–282.

Benamar A., Ammami M.T., Song Y., Portet-Koltalo F. (2020): Scale-up of electrokinetic process for dredged sediments remediation. Electrochimica Acta, 352: 136488.

Cameselle C. (2015): Enhancement of electro-osmotic flow during the electrokinetic treatment of a contaminated soil. Electrochimica Acta, 181: 31–38.

Chen J., Zhuang Y.F., Liu Z. (2025): Effect of electroosmosis flow and electrolyte circulation on electrokinetic remediation of Pb-contaminated kaolin. Journal of Applied Electrochemistry, 55: 259–272.

Chung H.I., Lee M.H. (2007): A new method for remedial treatment of contaminated clayey soils by electrokinetics coupled with permeable reactive barriers. Electrochimica Acta, 52: 3427–3431.

Diagboya P.N., Olu-Owolabi B.I., Adebowale K.O. (2015): Effects of time, soil organic matter, and iron oxides on the relative retention and redistribution of lead, cadmium, and copper on soils. Environmental Science and Pollution Research, 22: 10331–10339.

Duan Q., Lee J., Liu Y., Chen H., Hu H. (2016): Distribution of heavy metal pollution in surface soil samples in China: A graphical review. Bulletin of Environmental Contamination and Toxicology, 97: 303–309.

Gent D.B., Mark Bricka R., Alshawabkeh A.N., Larson S.L., Fabian G., Granade S. (2004): Bench- and field-scale evaluation of chromium and cadmium extraction by electrokinetics. Journal of Hazardous Materials, 110: 53–62.

Giannis A., Gidarakos E. (2005): Washing enhanced electrokinetic remediation for removal cadmium from real contaminated soil. Journal of Hazardous Materials, 123: 165–175.

Hou S., Zheng N., Tang L., Ji X., Li Y. (2019): Effect of soil pH and organic matter content on heavy metals availability in maize (*Zea mays* L.) rhizospheric soil of non-ferrous metals smelting area. Environmental Monitoring and Assessment, 191: 634.

Hu W., Cheng W.C., Wen S. (2023): Investigating the effect of degree of compaction, initial water content, and electric field intensity on electrokinetic remediation of an artificially Cu- and Pb-contaminated loess. Acta Geotechnica, 18: 937–949.

Li D., Tan X.Y., Wu X.D., Pan C., Xu P. (2014): Effects of electrolyte characteristics on soil conductivity and current in electrokinetic remediation of lead-contaminated soil. Separation and Purification Technology, 135: 14–21.

Li X., Yang Z., He X., Liu Y. (2020): Optimization analysis and mechanism exploration on removing cadmium from contaminated soil by electrokinetic remediation. Separation and Purification Technology, 250: 117180.

López Vizcaíno R., Yustres A., Asensio L., Saez C., Canizares P., Rodrigo M.A., Navarro V. (2018): Enhanced electrokinetic remediation of polluted soils by anolyte pH conditioning. Chemosphere, 199: 477–485.

Luo Y., Teng Y. (2020): Research progresses and prospects on soil pollution and remediation in China. Acta Pedologica Sinica, 57: 1137–1142. (in Chinese)

Murtaza B., Murtaza G., Zia-Ur-Rehman M. (2011): Reclamation of salt-affected soils using amendments and growing wheat crop. Soil and Environment, 2: 130–136.

https://doi.org/10.17221/140/2024-SWR

Ng Y.S., Sen Gupta B., Hashim M.A. (2014): Performance evaluation of two-stage electrokinetic washing as soil remediation method for lead removal using different wash solutions. Electrochimica Acta, 147: 9–18.

Ottosen L.M., Lepkova K., Kubal M. (2006): Comparison of electrodialytic removal of Cu from spiked kaolinite spiked soil and industrially polluted soil. Journal of Hazardous Materials, 137: 113–120.

Peng S., Wang P., Peng L. (2018): Predicting heavy metal partition equilibrium in soils: roles of soil components and binding sites. Soil Science Society of America Journal, 82: 839–849.

Song Y., Ammami M.T., Benamar A., Mezazigh S., Wang H. (2016): Effect of EDTA, EDDS, NTA and citric acid on electrokinetic remediation of As, Cd, Cr, Cu, Ni, Pb and Zn contaminated dredged marine sediment. Environmental Science and Pollution Research, 23: 10577–10586.

Villen-Guzman M., Garcia-Rubio A., Paz-Garcia J.M., Rodriguez-Maroto J.M., Garcia-Herruzo F., Vereda-Alonso C., Gomez-Lahoz C. (2015): The use of ethylenediaminetetraacetic acid as enhancing agent for the remediation of a lead polluted soil. Electrochimica Acta, 181: 82–89.

Wang Y., Li A., Cui C. (2021): Remediation of heavy metal-contaminated soils by electrokinetic technology: Mechanisms and applicability. Chemosphere, 265: 129071.

Xie N., Chen Z., Wang H., You C. (2021): Activated carbon coupled with citric acid in enhancing the remediation of Pb-contaminated soil by electrokinetic method. Journal of Cleaner Production, 308: 127433.

Yeung A.T., Gu Y.Y. (2011):A review on techniques to enhance electrochemical remediation of contaminated soils. Journal of Hazardous Materials, 195: 11–29.

Yuan L., Xu X., Li H., Wang Q., Wang N., Yu H. (2017): The influence of macroelements on energy consumption during periodic power electrokinetic remediation of heavy metals contaminated black soil. Electrochimica Acta, 235: 604–612.

Zhang J., Xu Y., Li W., Zhou J., Zhao J., Qian G., Xu Z.P. (2012): Enhanced remediation of Cr(VI)-contaminated soil by incorporating a calcined-hydrotalcite-based permeable reactive barrier with electrokinetics. Journal of Hazardous Materials, 239–240: 128–134.

Zhou D.M., Deng C.F., Cang L. (2004): Electrokinetic remediation of a Cu contaminated red soil by conditioning catholyte pH with different enhancing chemical reagents. Chemosphere, 56: 265–273.

Zulfiqar W., Iqbal M.A., Butt M.K. (2017): Pb^{2+} ions mobility perturbation by iron particles during electrokinetic remediation of contaminated soil. Chemosphere, 169: 257–261.

Received: November 14, 2024
Accepted: June 4, 2025
Published online: June 19, 2025